Engineering and Technology Journal
Journal homepage: https://etj.uotechnology.edu.iq

Experimental Investigation of Artificial Cavities Effect of Single-Phase Fluid Flow and Heat Transfer in Single Microchannel

Qahtan A. Al-Nakeeb*, Ekhlas M. Fayyadh , Moayed R. Hasan
Department of Mechanical Engineering, University of Technology-Iraq, Alsina'a street, 10066 Baghdad, Iraq.
*Corresponding author Email: qahtan.a.alnakeeb@uotechnology.edu.iq

HIGHLIGHTS

- The conventional correlation is appropriate for predicting the friction factor for smooth surface of microchannel.
- Developing heat transfer flow region is a dominated in microchannel within operating conditions.
- Enhancement of the heat transfer performance for the microchannel by using artificial nucleation sites.

ARTICLE INFO

Handling editor: Muhsin J. Jweeg
Keywords:
Microchannel; Single-phase flow; Friction factor; Nusselt number; Pressure drop.

ABSTRACT

In this paper, an experimental study has been conducted to investigate the influence of artificial cavities (artificial nucleation sites, ANS) in a single microchannel on the characteristics of flow and heat transfer at a single-phase flow. The experiments were performed with deionized water as a working fluid at 30^{O}C inlet temperature with a range (108.6-2372) of Reynolds numbers. Three models of the straight microchannel (model-1, model-2, and model-3) were manufactured of brass having a rectangular shape with a hydraulic diameter of (0.42 mm). Model-1 has a smooth surface, while model-2 has artificial cavities with a number of 40 ANS located on the base of the microchannel; along a line adjacent to one of the sidewalls. Also, the artificial cavities of model-3 exist at the base of the microchannel; along a line that is nearest to each sidewall for the microchannel. The number of ANS at each sidewall is 40 (i.e. the overall number of artificial nucleations is 80). The results manifested the enhancement of heat transfer by the presence of ANS for model-2 and model-3 as compared to model-1 by 15.53% and 16.67%, respectively. Also, the results proved that the fanning friction factor correlation for laminar and turbulent flow can predict very well the results (MAE=6.6-7.2%) and (MAE=4.1-7.7%), respectively. Also, the Nusselt number increases with increasing Reynolds number. However, the conventional correlation that predicted the experimental results is lower than the correlations (MAE=30.1%, 13.2% and 12.6%) for Model-1, -2 and -3, respectively.

1. Introduction

Aggressive miniaturization of electronic components has spurred an urgent need over the past three decades for more reliable thermal management technologies that could safely keep the system temperatures below specific material and performance limits. This pattern started mainly at the beginning of 1980 when a rapid escalation in the heat dissipation resulted in a change of the heat sink attachments cooling with a fan to a range of cooling systems by liquid. Initially, only a liquid was used which has been regarded as a solution in cooling single-phase flow [1].Several researchers have investigated the flow and heat transfer in microchannels. It was explained why some results differ from the conventional correlations represented as inlet effects, temperature dependent properties, compression effects, conjugated heat transfer, viscous heating, surface roughness, scaling effect, and experimental uncertainties. To date, it is not clear which variables influence the behavior of flow and heat transfer in microchannels. Some researchers reported that there was a deviation of heat transfer in microchannel from that of conventional theory and macroscale correlations. Harms et al. [2] performed an experimental investigation to study the single-phase forced convection for the deionized water flow through single and multiple deep rectangular silicon microchannels (having 251 µm width, 1 mm depth, and 119 µm channel wall thick) for a Reynolds number range (193-12900) based on the microchannel hydraulic diameter. For the case of a single microchannel, the experimental results of the Nusselt number were found to be higher than that of the predicted ones for all the flow rates considered. While for a multiple microchannel case, the Nusselt number was compatible with the conventional one only at the high flow rates. However, the limitation in the sizing of heat exchangers required the knowledge of its effect on the thermo-hydraulic characteristics in priori. Works related to the thermo-hydraulic performance of single phase microchannel heat exchangers were discussed by Qu and Mudawar, [3]. Experimental and numerical investigations of the pressure drop and the heat transfer characteristics of a single-phase laminar flow in a copper rectangular microchannel (having 0.231 mm width and 0.713 mm depth) and two heat flux values (100 W/cm^2 and 200 W/cm^2) for a Reynolds number range (139-1672) were performed. A good agreement was found between the measurements and numerical predictions, validating the use of the conventional Navier–Stokes equations for microchannels. However, some researchers studied also the effect of hydraulic diameter on the thermal performance, as Lee et al. [4], who

http://doi.org/10.30684/etj.v40i1.2122
Received 09 April 2021; Accepted 22 July 2021; Available online 25 January 2022
2412-0758/University of Technology-Iraq, Baghdad, Iraq

investigated the influence of the hydraulic diameters of copper microchannels on the thermal behavior of a single-phase flow using deionized water, the width of microchannel range was (194-534 μm). Experiments were performed at Reynolds numbers ranging from 300 to 3500. It was stated that the heat transfer coefficient increased with the decreasing of channel size, and the traditional correlations significantly deviated from the experimental results.

The effect of microchannels width on the friction factor and thermal behavior was investigated by Jung and Kwak, 2008 [5]. Experiments were performed for a silicon microchannel having the same length (15 mm) and depth (100 μm) with different widths (100 μm, 150 μm and 200 μm); using deionized water as working fluid. It was claimed that the heat transfer coefficient and wall temperature had a linear relationship. Also, the relation of the Nusselt number with the Reynolds number deviated from the conventional values obtained in the conventional case. However, the friction factor in a laminar flow was found to be compatible with traditional ones. García-Hernando et al. [6] investigated the effect of two scales of square stainless steel microchannel on the thermal and hydrodynamic performance, the hydraulic diameters of microchannel were (100 μm) and (200 μm). One of the scales was small hydraulic diameter, while the other was larger. Deionized water was used as a working fluid. It was concluded that the results did not deviate from the conventional ones. Also, no effect was observed for the microchannels having a small scale upon the heat transfer enhancement or the pressure drop increase.

Mirmanto et al. [7] studied the heat transfer and fluid flow characteristics of a single-phase flow for three single copper microchannels that have three different hydraulic diameters (438 μm, 561 μm and 635 μm) with various aspect ratios. Deionized water was used as a working fluid with a range (500-5000 $kg/m^2.s$) of mass. It was confirmed that the experimental friction factor and the Nusselt number values were higher than the conventional values for the fully developed condition. The experimental parameters, such as the influences of an entrance, the uncertainties of experiments, the losses of the inlet and exit pressure, and the leaving from laminar flow were taken into consideration in the experimental works. Results manifested that the developed equations for the traditional scale flow can be applied to the water flows which are in the experimental microchannel sizes. Lin and Kandlikar, [8] implemented the structured roughness influence upon the flow and heat transfer features at a microscale. The studied roughness variables were the relative roughness, the height of roughness, and the element pitch of roughness. Eight single channels having a rectangular shape and made from stainless steel with various hydraulic diameters (from 710 μm to 1870 μm) and a relative roughness range (0-96 μm) were tested by utilizing water as working fluid. The results of the Nusselt number of smooth channels were foreseen properly with a conservative correlation in the developing as well as the fully developed flow. It was obtained that the coefficient of heat transfer improved via the structure of roughness. Nevertheless, the surface having a higher relative roughness possessed a bigger value in the drop of pressure and the heat transfer. Moreover, the premature transition was from the laminar to the turbulent flow. Also, it was documented that the element pitch of roughness didn't influence the heat transfer in the investigation range.

Salem et al. [9] investigated a group of experimental works by using circular stainless steel microchannel (850 μm in diameter) to study the effect of surface roughness on the friction factor and heat transfer using two different working substances (distilled water and R134a), and the range of Reynolds number was (100-10000). It was discovered that the data results presented a better covenant with the macro-scale theory for a laminar zone for the results of friction factor and the values of Nu, even though the premature transition was detected. So, the friction factor results for a turbulent region can be foreseen properly by the macro-scale theories, but the measured values of Nu were lesser than those foreseen by correlations. Tamayol et al. [10] studied experimentally the influence of array micro-cylinders that are embedded in silicon microchannels surfaces on the fluid flow resistance for predicting the fluid flow resistance analytically; the hydraulic diameter of microchannel was 363 μm and using nitrogen as a working fluid. (2) methods were employed in the experimental work; the first method was using a porous medium, while the other approach was using a changeable cross-section of channels. A relation of the drop of pressure stated in terms of geometrical factors (i.e. the diameter of the micro-cylinder, the spacing between neighboring cylinders, and the geometry of the channel (the width and height of channel)). The results evinced that these methods captured the investigational work tendency. The changeable cross-section method was highly precise for the geometries, where the gap spacing ratio to the size of the cylinder and the height of the channel being slight, but it appears less precise as the structure's porosity and the sizes of gaps raise, whereas the process of porous medium manifested a sensible precision. Nevertheless, the authors proposed that an optimum diameter of the micro-cylinder does exist for minimizing the drop of pressure, which the diameter being a function of the geometries of the channel as well as the required ratio of the surface area to volume.

In addition, the influence of surface roughness was investigated via Xing et al. [11] by using (3) stainless steel circular microchannels possessing various surface roughnesses (0.86 μm, 0.92 μm, and 1.02 μm) but with a similar diameter (400 μm). The air was used as a working fluid with a range of Reynolds numbers (150-2800). It was detected that the highly relative roughness caused higher values of Poiseuille and Nu. Also, the friction factor value was reduced with the Re increase. In contrast, the value of Nu was rising with the raising the values of Re. Moreover, the authors discovered that the earlier transition from laminar to the turbulent regime is at Re = 1500.

The influence of aspect ratio for micro-channel having the same hydraulic diameter on the friction factor and heat transfer was investigated by Markal et al. [12]. Experiments were performed in a multi microchannel using deionized water as a working fluid with a Reynolds number range (12.3-47.3). The experimental results elucidated that as the aspect ratio increases; the Nu increased and decreased the friction factor. Also, the experimental Nu as well as the friction factor was obtained to be lower than the traditional correlations. Kumar et al. [13] conducted experiments in a single-phase flow to investigate the friction factor and Nu inside ten copper semi-circular multi microchannels having a hydraulic diameter of (214 μm) and a length of 60 mm, using de-ionized water as a working fluid. The obtained experimental outcomes obtained displayed a good agreement with the conventional theory of hydraulic flow, and it was also found that the flow within the microchannels was a fully developed laminar flow. However, at a lower Reynolds number, it was observed that the experimental values of Nu differ slightly from the traditional correlations. Huang et al. [14] investigated experimentally the effect of cavities on the single-phase heat transfer and pressure drop. The experimental work was done as a ten silicon multi-microchannel having a 300 μm

hydraulic diameter and a 40 mm length. The experiment was performed at a low Reynolds number. The results pointed out that, as compared with the traditional microchannel, adding cavities in microchannels could attain the heat transfer enhancement and the pressure drop reduction together. Mohammed and Fayyadh, [15] performed an experimental investigation to study the effect of artificial cavities on the friction factor and thermal behavior in a square copper single microchannel heat sink having a 300 μm hydraulic diameter. The experiments were performed at two models (model-1and model-2) of straight microchannel having the same hydraulic diameter. Model-1 was without artificial cavities, while Model-2 had (47) artificial cavities uniformly distributed along the bottom surface of the microchannel longest. De-ionized water was utilized as the operating fluids. Experimental outcomes elucidated that the experimental friction factor could be predicted well with the conventional correlation of developing flow in the laminar region for the two models. As well, the investigational Nu agrees properly with the conventional and microchannel correlations in the laminar region.

Obviously, there are two methods for enhancing the heat transfer in the channel; the first method is changing the surface roughness of the channel through using a milling machine, while the other method was artificial roughness, such as a micro-pin, artificial cavities and reentrant cavities. As a result, it was found that using the artificial roughness method can enhance the heat transfer more than the machining roughness. Moreover, some researchers agreed with the experimental results for the flow and heat transfer in microchannels with the conventional correlations, while the others disagreed with the conventional correlation. Actually, till now, it is not clear exactly the variables that influence the behavior of flow and heat transfer in microchannels. So, in this paper, an experimental study was carried out to investigate the effect of location and distribution of artificial cavities upon the flow and heat transfer characteristic in a single microchannel and compare the predicted friction factor and Nu with the experimental data, conventional, and micro-scale correlations.

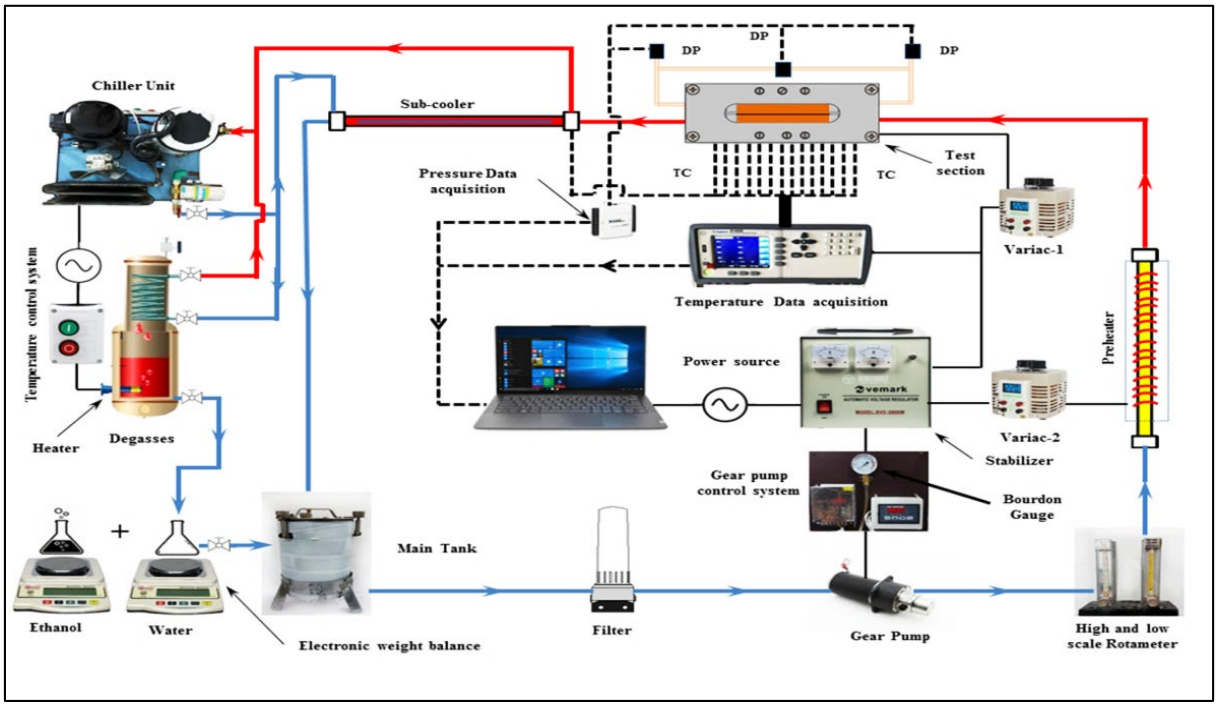

Figure 1: Schematic diagram of the experimental setup

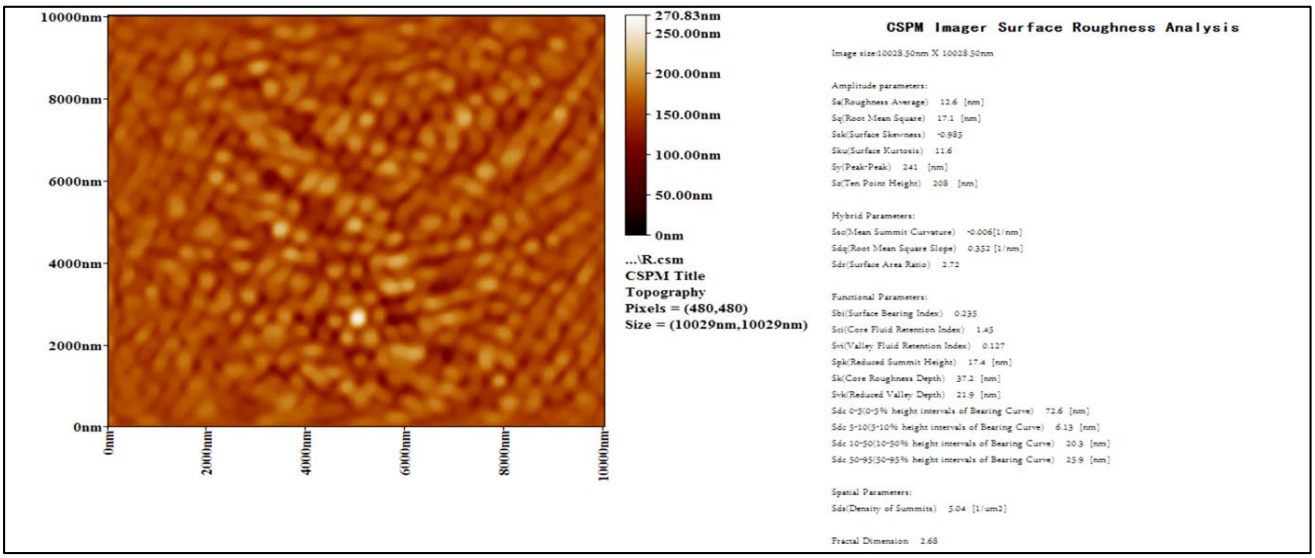

Figure 2: Surface roughness analysis of microchannel bottom of a sample

2. Experiment Setup

The experimental setup consists of an in-line filter, a micro gear pump, a preheater, a sub-cooler, a test section, and a tank of deionized water. Low rotameter (model LZB-3WBF), medium rotameter (CX-GRM-LZB-4WB) and high rotameter (LZB-4WB) were employed for the experimental works. They were calibrated with an accuracy of (± 0.32 ml/min), (± 0.55 ml/min), and (± 0.425 ml/min), respectively. The condenser and sub-cooler utilize a chiller unit for the purposes of cooling. Plate 1 and Figure 1 view the experimental setup and the schematic diagram, correspondingly. To degas the deionized water inside the tank of liquid, a concentrated boiling for about (1 hr) was done. The condenser's upper valve was opened to release the incondensable gases to the surrounding. A filter of (5 μm) was fixed before the gear pump at the location for removing the whole particles from water. Then, throughout the pumping, the water that became degassed was introduced in the test section, and a preheater was utilized for regulating the working fluid's inlet temperature.The test section comprises a Brass-block (61.48 wt% of Cu and 38.52 wt% of Zn) which possesses one micro-channel at the upper surface, polycarbonate housing, cartridge heaters, and an upper cover plate. A single-rectangular micro-channel was cut into the Brass-block's top surface via a milling machine at a feed rate of (10 mm/min). The Brass-block dimensions were (60 mm) in length, (12 mm) in width, and (60 mm) in height. The micro-channel nominal dimensions were (0.3 mm) in width and (0.7 mm) in depth. The real depth and width values of the single micro-channel which were evaluated via scanning electronic microscope (SEM) were (665.6 μm) and (325.25 μm), correspondingly; see Figure (4), the microchannel's bottom surface roughness being measured by AA3000 scanning probe microscope (atomic force microscope (AFM) contact mode), which scanned over an area (10028.5 nm x 10028.5 nm) and evaluated the average roughness (equal to 12.6 nm), as shown in Figure 2. For supplying a heat power that utilized to heat the Brass-block, a pair of cartridge heaters having a (100 W) heat power each was horizontally introduced at the Brass-block's bottom, as depicted in Figure 3. (4) thermocouples (type-K) were vertically introduced alongside the brass-block centerline with an equidistance of (14.7 mm) for measuring the temperature of a block, and that helps compute the heat flux. For calculating locally the heat transfer coefficient alongside the channel length in the axial direction, (7) thermocouples (type-K) were positioned at (1 mm) beneath the channel and spread alongside the channel axial direction with an equidistant of (9.67 mm). The diameter of all thermocouples used in the Brass-block was (0.5 mm). The thermocouple calibration accuracy was around (± 0.5 K). The Brass-block was introduced into the polycarbonate housing and sealed utilizing O-rings, as revealed in Figure 3. This polycarbonate housing of polycarbonate comprises the inlet/outlet manifolds as well as sub-channels, which connected the inlet/outlet manifolds to the micro-channel. The thermocouples (type-K) having a 0.5 mm diameter was inserted into the inlet-out manifolds for measuring the fluid inlet-outlet temperature and were calibrated with (± 0.5 K) accuracy. The fluid pressure at the inlet-outlet manifolds being measured employing the transducers (model MPX5500DP) of absolute pressure, which were calibrated with a (±2.13 kPa) accuracy. The drop of pressure across the test section was measured straight utilizing differential pressure a transducer (model MPX4250DP) of differential pressure, which was calibrated with a (±1.17 kPa) accuracy. The inlet and outlet manifolds have a height of (10 mm) width of (20 mm), and a depth of (10 mm) depth, whereas the inlet-outlet sub-channels have a length of (7 mm), a width of (2 mm), and a depth of (0.7 mm). The thermocouples wires at the Brass-block pass-through holes in the polycarbonate housing. The hole's diameter was (0.9 mm) and its number is equivalent to the number of thermocouples. The polycarbonate layer with a (6 mm) thickness was sandwiched between the upper polycarbonate cover plate and the housing upper surface. To prevent any leakage from the upper surface of the housing, a polycarbonate layer was sealed by employing the O-ring set in the housing on its upper surface. As evinced in plate 2, an envisaged window was generated at the upper cover plate with a similar dimension as the block of micro-channel, comprising the sub-channels. The temperature data were registered to utilize a data logger reading (Applent AT 4532x). Bus-power multifunction DAQ USB (model NI USB-6009) was employed as an interface apparatus for compiling the signals (0-5 DC–Volt) of the transducer of pressure from the gauges of the pressure of the transducer to the program of LabView**.** The data of the experiment were read as well as registered by the (NI USB-2009) and program of LabView at a (1 msec) interval time. Tests were conducted by protecting the rate of flow invariable and continuously raising the power of supply. Data were first gathered throughout (3 min) and after that summed to be utilized in the data decreasing procedure. However, three different models of single rectangular microchannel were manufactured, as shown in plate 3. The first model (model-1) of the microchannel is a conventional brass surface (without drilled artificial nucleation sites, ANS); meanwhile, the second model (model-2) and third model (model-3) of microchannel have ANS with 50 μm diameter. However; the artificial nucleation of model-2 is located at the base of the microchannel and along a line adjacent to its sidewall with a number of 40. Whilst, the artificial nucleation of model-3 is existed also at the base of the microchannel and along a line adjacent to each sidewall. The number of ANS close to each sidewall is 40 (i.e. the overall number of ANS is 80). The first nucleation site for model-2 and model-3 was located by the entrance of the microchannel at distance equal to 1/3 of the microchannel length. The interval distance between artificial nucleation site centers is regular with a value of 1 mm.

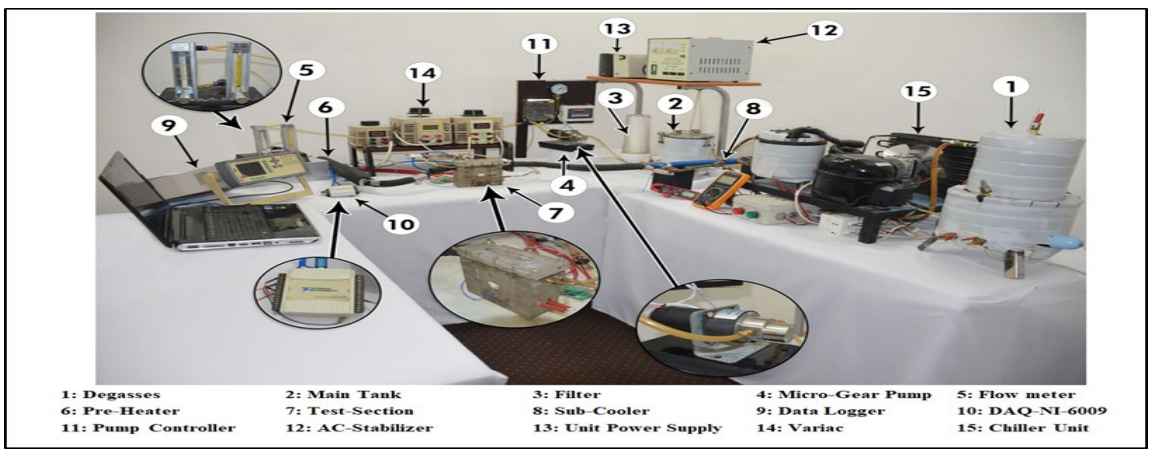

Plate 1: The experimental setup

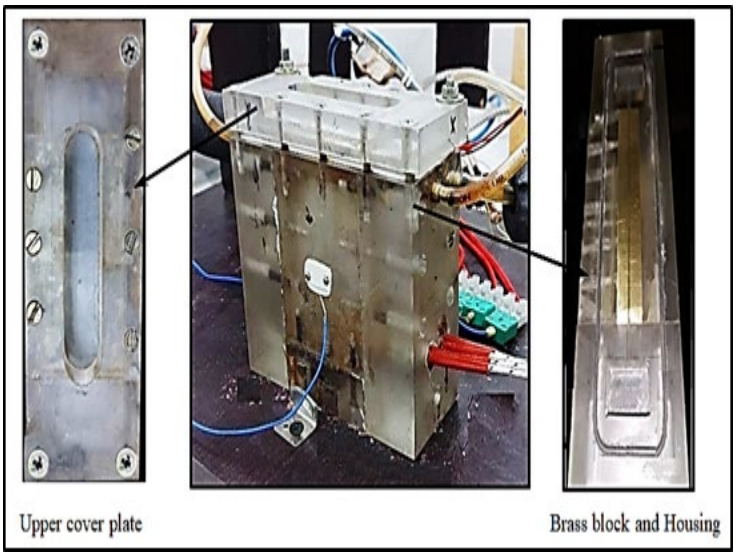

Plate 2: The test section

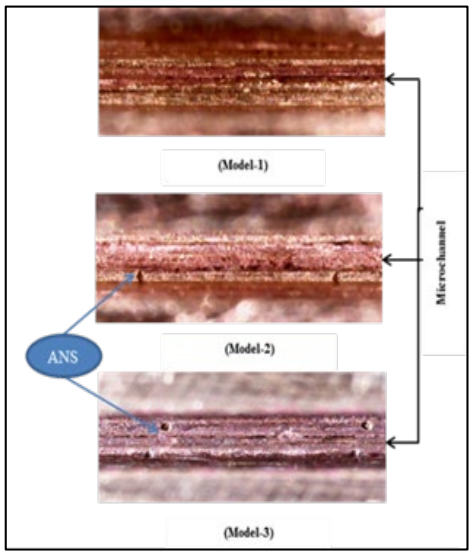

Plate 3: The michrochannels models

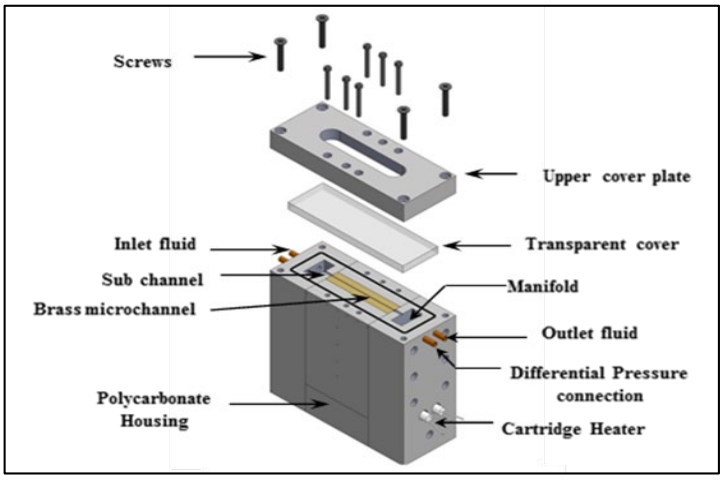

Figure 3: Schematic of the Test section

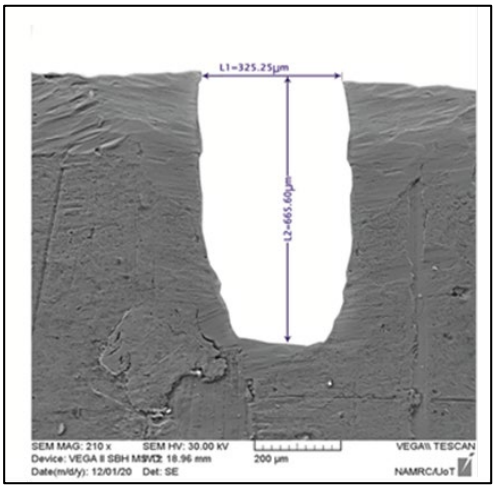

Figure 4: Actual dimensions of microchannel

3. Phase Data Reduction

The net drops of pressure for the single-flow alongside the micro-channel (ΔP_{ch}) are stated via [16]:

$$\Delta P_{ch} = \Delta P_m - \Delta P_{loss} \quad (1)$$

Where: ΔP_m: The entire measured drop of pressure

ΔP_{loss}: The entire losses of pressure owing to the drop of pressure in the inlet subchannel ($\Delta P_{sch,i}$) the outlet sub-channel ($\Delta P_{sch,o}$), the abrupt contraction (ΔP_{sc}), and abrupt expansion (ΔP_{se}), as written below [17]:

$$\Delta P_{loss} = \Delta P_{sch,i} + \Delta P_{sch,o} + \Delta P_{sc} + \Delta P_{se} \quad (2)$$

The contribution of losses due to the inlet/outlet sub-channel at the ultimate Re no. (2372) was (0.42%) and at the minimum Re no. (108) was (0.33%), therefore, it was neglected. Thus, the losses of pressure owing to the abrupt contraction and expansion were computed, as given via this formula [17]:

$$\Delta P_{loss} = (K_{sc1} + K_{se2}).\frac{V_{sch}^2 \cdot \rho}{2} + (K_{sc2} + K_{se1}).\frac{V_{ch}^2 \cdot \rho}{2} \quad (3)$$

In the abovementioned expression, (K_{sc1}) and (K_{sc2}) are the loss coefficients of the abrupt contraction from the manifold to the sub-channel as well as from the subchannel to the microchannel, correspondingly, whereas (K_{se1}) and (K_{se2}) are the loss coefficients of the abrupt expansion from the micro-channel to the subchannel as well as from the subchannel to the manifold. The loss coefficients (K_{sc1}, K_{sc2}, K_{se1}, and K_{se2}) values are obtained as (0.5, 0.47, 0.72, and 0.81), correspondingly [18]. The fanning friction factor (f) is defined as the ratio of wall shear stress (τ) to the kinetic energy per unit volume ($\rho V_m^2/2g$) [19]. So, the experiment fanning friction factor based on the microchannel pressure drop can be evaluated by equation bellow[16]:

$$f_{ch} = \frac{\Delta p_{ch} D_h}{2L\rho V_{ch}} \quad (4)$$

The supplemented heat flux to the test section ($q_b^{"}$)was computed via the balance of energy [16] as:

$$q_b^{"} = \frac{P - Q_{loss}}{A_b} \quad (5)$$

$$P = IV \quad (6)$$

Where:

A_b: The heat sink base area. This is computed with the base heated width (W) as well as the heated length (L_{ch}) on the base block as given in this equation:

$$A_b = W.L_{ch} \quad (7)$$

Q_{loss}: The test section heat loss to the surrounding and assessed via heating the section with no liquid pumping.

If the system was steady, the power would be registered. Such a process was repeated. Eventually, the loss of power is connected with the difference of temperature between ambient and test section for various system temperature and power values. Such a technique was implemented via numerous investigators [15, 20].

The local coefficient of heat transfer ($h_{sp}(z)$) is obtained by this equation [16]:

$$h_{sp}(z) = \frac{q_b^{"} W}{(T_W(z) - T_f(z))(W_{ch} + 2H_{ch})} \quad (8)$$

W_{ch} and H_{ch} are respectively the width and height of the channel. The local thermocouples were inserted at a distance (*th*) of 1 mm from the bottom of the microchannel. Thus, the temperature values of thermocouples ($T_{tc}(z)$) were amended using the one-dimensional heat conduction formula to evaluate the value of the inner surface of microchannel temperature ($T_w(z)$), as expressed by equation [16] below:

$$T_W(z) = T_{tc}(z) - \frac{q_b^{"} th}{K_s} \quad (9)$$

If the consistent boundary condition is assumed, the local temperature of the fluid ($T_f(z)$) can be computed via the following formula [16]:

$$T_f(z) = T_i + \frac{q_b^{"} W.z}{\dot{m} C_p} \quad (10)$$

Where: T_i, C_p , and $\dot{m}$: The inlet temperature of the fluid, fluid specific heat, the rate of mass flow, respectively.

Z: The axial site of the length of the channel

The average Nu no. being given via [16]:

$$Nu = \frac{1}{L_{ch}} \int_0^{L_{ch}} \frac{h_{sp}(z).D_h}{K_l} dz \quad (11)$$

Experimental data were conducted at a (1 atm) system pressure, a (70.154 kW/m^2) heat flux, a range of Re no. (108.6-2372), and using deionized water as working fluid. The spread uncertainty in friction factor and the coefficient of heat transfer was computed in accordance with the technique as reported by [21]**,** and the values were 5.5–8.2%, 7.2–8.7% and 4.1-63.2%, respectively, see Table 1.

Table 1: Uncertainties for the single-phase heat transfer experiments

Parameter	Uncertainty
Hydraulic diameter, *Dh* (mm)	±3.0%
Heat transfer area A_{ht} (mm)	±2.16%
Mass flux, *G* (kg/m^{2}s)	±4.9-16.6%
Channel fanning friction factor, *fch*	±4.1-63.2%
Heat flux, *q"* (kW/m^2)	±5.5-8.2 %
Average heat transfer coefficient, *hsp* (kW/m^{2}K)	±7.2-8.7%
Average Nusselt number, *Nu*	± 7.2-8.7%

4. Results and Discussion

4.1 Single phase Validation

Single-phase experiments were performed at a system pressure of 1 bar at a range of Reynolds number for the adiabatic and diabatic conditions to verify all the instruments work properly within reasonable accuracy before starting the experiments. These experiments were carried out using deionized water as working fluid for three models, (i.e. test section of model-1, model -2, and model-3), at the inlet fluid temperature of (30°C) for the range of Reynolds number based on the hydraulic diameter of (108.6-2372). The results of the experimental work were compared to established correlations for calculating the friction factor and Nusselt number. These correlations were proposed for both conventional channels and microchannels. These correlations were evaluated using the mean absolute error (MAE) as follows:

$$MAE = \frac{1}{N}\sum_{j=1}^{N}\frac{|\emptyset_{pred,j}-\emptyset_{exp,j}|}{\emptyset_{exp,j}} * 100\% \quad (12)$$

4.1.1 Fanning friction factor *(f)* correlation

The experimental results of *(f)* for three models (1, 2, and 3) were compared with the Shah and London correlation for developing as well as fully developed flow in a zone of laminar flow. Thus, the apparent friction factor (f_{app}) for the developing flow at laminar region was calculated using the correlation of Shah and London, [19] as follows:

$$f_{app} = \frac{3.44}{Re(L^*)^{1/2}} + \frac{(f_{FD}Re)+\frac{K(\infty)}{4L^*}-\frac{3.44}{(L^*)^{1/2}}}{Re(1+C(L^*)^{-0.2})} \quad (13)$$

$$L^* = L_{sp}/ReD_h \quad (14)$$

Where $K(\infty)$ and C are constants, they depend on the aspect ratio for the present investigation, the values being ($1.7784x10^{-4}$), and (1.1962). And, the Poiseuille no. ($f_{FD}Re$) for a fully developing single-phase fluid was expressed via [19]:

$$(f_{FD}Re) = 24\begin{pmatrix}1-1.35534\beta+1.9467\beta^2-1.7012\beta^3\\+0.9653\beta^4-0.2537\beta^5\end{pmatrix} \quad (15)$$

$$\beta = \frac{w_{ch}}{H_{ch}} \quad (16)$$

Also, it was compared with the correlations of Phillis and Blasius [22] for developing and developed flow in a turbulent flow region. So, the Blasius Correlation of *(f)* for a fully developed turbulent flow is given as [19]:

$$f_{FDturb.} = 0.079Re^{-0.25} \quad (17)$$

Also, *(f)* for a developmental turbulent flow was expressed via [22]:

$$f_{appturb.} = \left(0.0929 + \frac{1.0161D_h}{L}\right)Re^{*\left(-0.268-\frac{0.3193D_h}{L}\right)} \quad (18)$$

Where Re^* is the equivalent Re no. that can be computed as:

$$Re^* = Re\left(2/3 + \frac{11}{24}\beta(2-\beta)\right) \quad (19)$$

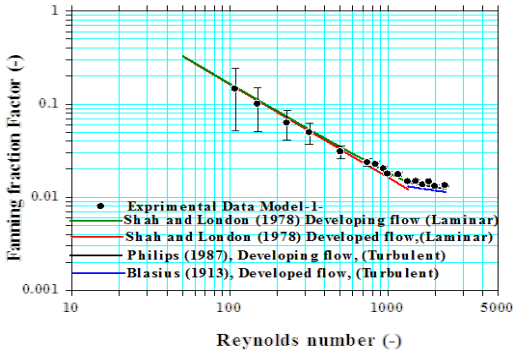

Figure 5: The experimental results of the fanning friction factor in comparison with the correlations of the laminar and turbulent flow for model-1

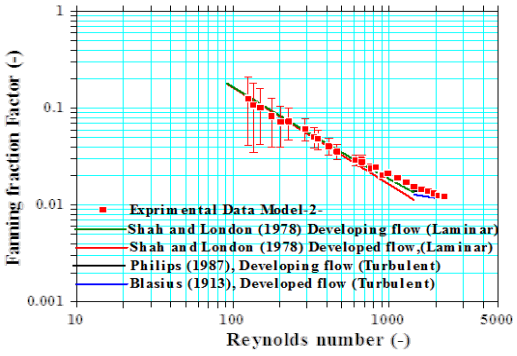

Figure 6: The experimental results of the fanning friction factor in comparison with the correlations of the laminar and turbulent flow for model-2

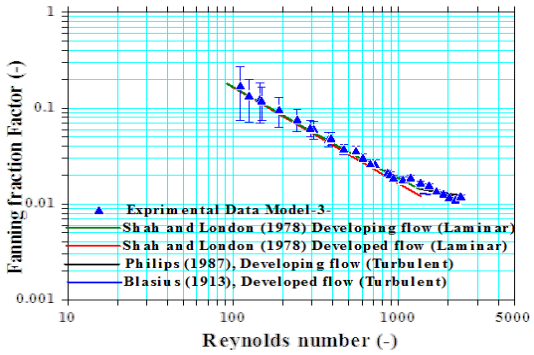

Figure 7: The experimental results of the fanning friction factor in comparison with the correlations of the laminar and turbulent flow for model-3

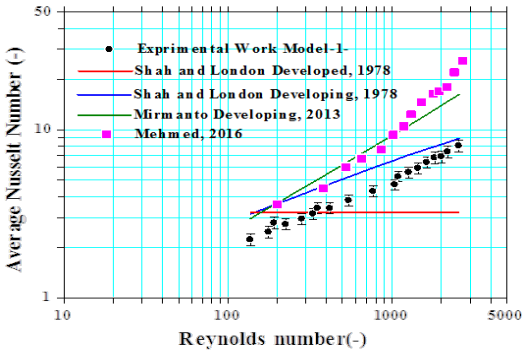

Figure 8: The experimental results of the average Nusselt number in comparison with the correlations of laminar flow for model-1

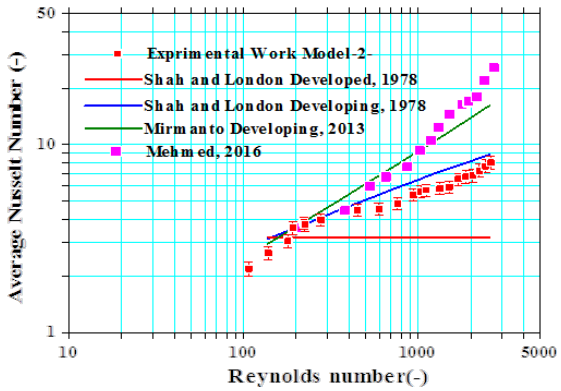

Figure 9: The experimental results of the average Nusselt number in comparison with the correlations of laminar flow of model-2

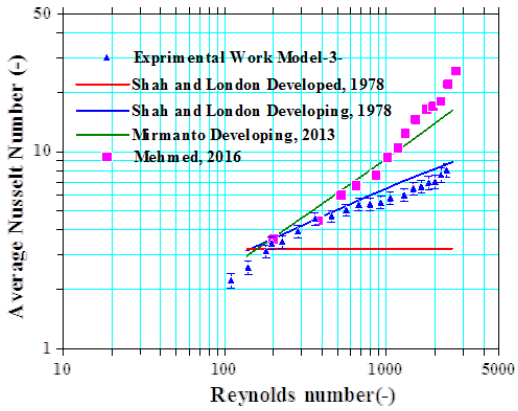

Figure 10: The experimental results of the average Nusselt number in comparison with the correlations of laminar flow for model-3

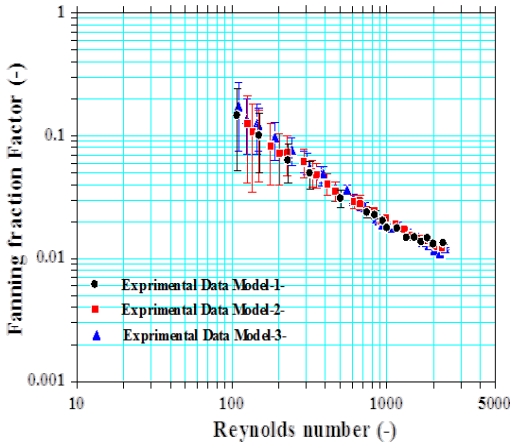

Figure 11: Effect of artificial cavities (model-2 and Model-3) on the fanning friction factor

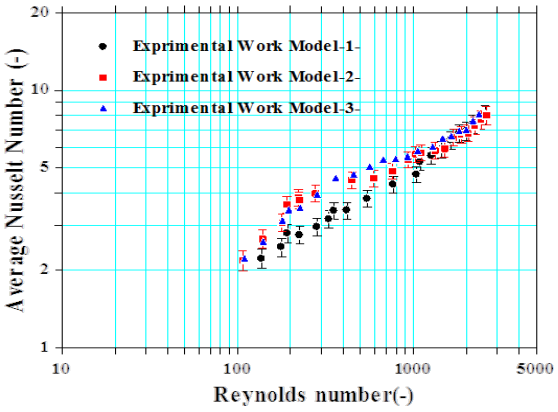

Figure 12: Effect of artificial cavities (model-2 and Model-3) on the average Nusselt number

The experimental fanning friction factor versus Reynolds number for three models is shown in Figures 5-7. From these figures, the comparison with the results of the three models manifests that the correlation between Shah and London in a laminar developed flow predicted the data with the mean absolute error (MAE) of 10.15%, 10.5% and 11.62% for model-1, model-2 and model-3, respectively. Meanwhile, in the laminar developing flow, the correlation Shah and London gave a reasonable agreement with a mean absolute error (MAE) of 7.2%, 6.9%, and 6.6% for model-1, model-2, and model-3, respectively. However, the correlation Blasius predicted the experimental results of the three models in the turbulent region are fully developed with the mean absolute error (MAE) of 13.45%, 11.62% and 9.8 % for model-1, model-2 and model-3, respectively. While in the turbulent developing flow, the correlation Phillips evinced a good prediction with a mean absolute error (MAE) of 5.23%, 4.1%, and 7.76% for model-1, model-2, and model-3, respectively. This agrees with the previous researchers, such as Qu and Mudawar, [3], Jung and Kwak, [5], García-Hernando et al. [6], Mirmanto et al. [7], Lin and Kandlikar, [8], Salem et al. [9], Kumar et al. [13] and Mohammed and Fayyadh, [15]. Generally, these results point out that the conventional theory is appropriate to predict the single-phase flow friction factor in these models of microchannels and at these experimental conditions.

4.1.2 Nusselt number correlations

Average Nusselt number results for three models were calculated and compared with the existing correlations for the conventional channels Shah and London [19] for a fully developed laminar flow equation which is given as:

$$Nu = 8.235\begin{pmatrix} 1 - 10.6044\,\beta + 61.1755\ \beta^2 \\ -155.1803\,\beta^3 + \\ 176.9203\beta^4 - 72.9236\,\beta^5 \end{pmatrix} \tag{20}$$

Where the Shah and London (1978) correlation of Nusselt number for a developing laminar flow [19] was formulated as:

$$Nu = 0.775\ L_t^{*(-1/3)}(fRe)_{FD}^{(1/3)} \quad (21)$$

Where L^* is a dimensionless channel length that can be denoted via this expression [19]:

$$L^*_t = \frac{L}{Re\ Pr\ D_h} \quad (22)$$

And, with the correlation of Mirmanto, [23] for a microchannel at a laminar region developing flow, L^* is given in this equation:

$$Nu = Re^{0.283} Pr^{-0.513} L_t^{*-0.309} \quad (23)$$

The experimental average Nusselt number versus Reynolds number for three models (1, 2 and 3) in the laminar regions are depicted in Figures 8, 9 and 10, respectively. It is clear that the trend curves of the experimental average Nusselt number for the three models are similar to the developing flow of the existing correlations, i.e. the average Nusselt number increases with Reynolds number for all models. This is caused by the thin thermal boundary layer in the thermally developing region that increased the heat transfer compared to the thermally fully developed region in the laminar regime. The entrance length of the thermally developing region can be determined using the Shah and London [19] equation as:

$$L_{th} = 0.056 Re D_h Pr \quad (24)$$

It is clear that the thermal entrance length is increased with increasing Reynolds number and can occupy the total channel length at Reynolds number around 600.

However, the comparison of the Shah and London correlations for a developmental flow with the results of model-1 exhibited a poor prediction with an MAE of 30.1%, this agrees with Harms et al. [2], Lee et al. [4], Jung and Kwak, [5], Salem et al. [9], Markal et al. [12] and Huang et al. [14]. While, a good agreement was getting for model-2 and model-3 with an MAE of 13.2% and 12.6%, respectively. Meanwhile, the correlation by Mirmanto manifested poor prediction results with a mean absolute error of 72.3%, 51.3% and 55.3% for model-1, model-2 and model-3, respectively. This deviation could be referred to the low thermal conductivity surfaces, for all models that were manufactured from the brass surface. Thus, this correlation was not taking the material effect into consideration.

In conclusion, it is clear that the experimental results in a single-phase flow confirm that the calibration and measurement system can provide accurate results for the two-phase flow experiments.

4.2 Effect of artificial cavities on the friction factor and Nusselt number

The artificial cavity effect upon the friction factor and Nusselt number is discussed and presented for the range of Reynolds number in this section. The effects of numbers and distributions of artificial cavities on the fanning friction factor are presented in Figure 11 for the range of Reynolds number (108.6-2372). From this figure, it is observed that the fanning friction factor for models with artificial cavities (model-2 and model-3) has the same behavior as compared to the smooth surface (model-1), where decreasing the fanning friction factor with increasing Reynolds number. That is due to the excess of inertia force than shear force when the Reynolds number is increased. Also, the figure depicts that the fanning friction factor for microchannel with the presence of artificial cavities (model -2, and model -3) is higher than that for the smooth microchannel (model-1) with (16.94% and 33.08%), respectively. Additionally, it was observed that increasing the number of artificial cavities at the bottom of the microchannel from 40 (model-2) to 80 (model-3) has a slight effect on the single-phase fanning friction factor based on these results. Nevertheless, Figure 12 elucidates the effect of the number of artificial cavities and its distribution at a bottom surface of the single microchannel (model-2 and model-3) on the single phase heat transfer performance as compared with the smooth surface (model-1) for the range of Reynolds number (109.2-2599). This figure displays that the heat transfer performance of the the microchannel models with the presence of artificial cavities (model-2, and model-3) is higher than the smooth surface of microchannel (model-1) with (15.53% and 16.67%), respectively. This indicated that the presence of artificial cavities leads to enhance heat transfer due to increasing the surface area, mixing and recirculation of the fluid flow which agrees with Huang et al. [14] and Mohammed and Fayyadh, [15]. However, no significant effect of the distribution and increasing the number of artificial cavities on the value of the average Nusselt number can be identified based on these results.

5. Conclusion

The experimental work was carried out for a single horizontal microchannel at a single-phase flow. So, the tests obtained are to identify the difference between the present experimental theoretical outcomes. Furthermore, the artificial cavities' influence and their distribution and position on the friction factor and heat transfer were investigated. Thus, the significant results that can be attained from the investigation include:

1) The outcomes demonstrated that the traditional correlation is appropriate for predicting the friction factor for three models (1, 2, and 3) for a developmental flow at a laminar region with the mean absolute error (MAE) of (7.2%, 6.9%, and 6.6%), respectively. Also, the mean absolute error (MAE) at a turbulent region for the same models is (5.23%, 4.1% and 7.76%), respectively.
2) The fanning friction factor for the models with the presence of artificial cavities (model-2 and model-3) is greater than that for model -1 with 16.94% and 33.08%, respectively.
3) The mean Nu no. rises with the increasing of Re no. for the (3) models conversely to the fully developed heat transfer.
4) The conventional correlation for a developing laminar flow is highly under predicted for the model-1 with a mean absolute error of 30.1%, but this correlation agrees very well with models 2 and 3 at a mean

absolute error of 13.2% and 12.6%, respectively. While, the microscales correlation is highly under predicted from models 1, 2, and 3 with a mean absolute error of 72.3%, 51.3% and 55.3%, respectively.

5) There's an improvement of the heat transfer performance for the models with the existence of artificial cavities (model-2, and model-3) as compared to the smooth model (model-1) with a value of about (15.53% and 16.67%), respectively, i.e. there is no a significant enhancement for the model-3 compared with the model-2 for the single-phase deionized water fluid flow.

NOMENCLATURE

A	Area, m²	Δ	Difference, drop
C	Constant	μ	Viscosity, kg/m.s
C_p	Specific heat at a constant pressure, J/kg. K	**Subscripts**	
D_h	Hydraulic diameter (m)	a	Ambient
$f_{FD}Re$	Poiseuille number for fully developed flow	*app*	Apparent
f	Fanning friction factor	Avg.	Average
G	Mass flux, kg/m² s	b	Base
H	Heat transfer coefficient, W/m² K	ch	Channel
H	Channel depth, m	Cu	copper
L	Channel length, m	br	brass
I	Current, A	*f*	Fluid
K	Thermal conductivity, W/m K	*FD*	Fully developed flow
$\dot{m}$	Mass flow rate, kg/sec.	e	Exit
N	Total number of data points	g	Gas, vapour
Nu	Nusselt number	ht	Heat transfer
P	Power, Watt	*i*	Inlet
P	Pressure, Pa	*l*	Liquid
Pr	Prandtl number	m	Measured
q"	Heat flux, W/m²	o	Outlet
Q_{loss}	Heat loss, Watt	sp	Single-phase
Re	Reynolds number	sch	Sub-channel
Re*	Equivalent Reynolds number	se	Sudden expansion
Th	Distance between thermocouple location and channel base, m	tc	Thermocouple
T	Temperature, °C	tub	Turbulent
V	Voltage, V	w	Wall
V	Velocity, m/s	Zn	Zinc
W	Width, m		
Z	Distance measured from inlet channel, m	**Abbreviations**	
Greek Symbols		ANS	Artificial Nucleation site
β	Aspect ratio	MAE	Mean absolute error
δ_{th}	Thermal boundary layer thickness, m	SEM	Scanning electron microscopy
ø	Fanning friction factor or Nusselt number parameter		

Author contribution

All authors contributed equally to this work.

Funding

This research received no specific grant from any funding agency in the public, commercial, or not-for-profit sectors.

Data availability statement

The data that support the findings of this study are available on request from the corresponding author.

Conflicts of interest

The authors declare that there is no conflict of interest.

References

[1] I. Mudawar, Recent advances in high-flux, two-phase thermal management, J. Therm. Sci. Eng. Appl., 5 (2013) 1-15. https://doi.org/10.1115/1.4023599

[2] T. M. Harms, M. J. Kazmierczak, F. M. Gerner, Developing convective heat transfer in deep rectangular microchannels, Int. J. Heat Fluid Flow, 20 (1999) 149 –157. https://doi.org/10.1016/S0142-727X(98)10055-3

[3] W. Qu, I. Mudawar, Experimental and numerical study of pressure drop and heat transfer in a single-phase micro-channel heat sink, Int. J. Heat. Mass. Transf., 45 (2002) 2549–2565. https://doi.org/10.1016/S0017-9310(01)00337-4

[4] P. S. Lee, S. V. Garimella, D. Liu, Investigation of heat transfer in rectangular microchannels, Int. J. Heat. Mass. Transf., 48 (2005) 1688–1704. https://doi.org/10.1016/j.ijheatmasstransfer.2004.11.019

[5] J. Y. Jung , H.Y. Kwak, Fluid flow and heat transfer in microchannels with rectangular cross section, Heat Mass Transf., 44 (2008) 1041–1049. https://doi.org/10.1007/s00231-007-0338-4

[6] N. García-Hernando, A. Acosta-Iborra, U. Ruiz-Rivas, M. Izquierdo, Experimental investigation of fluid flow and heat transfer in a single-phase liquid flow micro-heat exchanger, Int. J. Heat. Mass. Transf., 52 (2009) 5433–5446. https://doi.org/10.1016/j.ijheatmasstransfer.2009.06.034

[7] Mirmanto, D. B. R. Kenning, J. S. Lewis,T. G. Karayiannis, Pressure drop and heat transfer characteristics for single-phase developing flow of water in rectangular microchannels, J. Phys. Conf. Ser., 395 (2012) 012085. https://doi.org/10.1088/1742-6596/395/1/012085

[8] T. Y. Lin , S. G. Kandlikar, An experimental investigation of structured roughness effect on heat transfer during single-phase liquid flow at microscale, J. Heat. Transfer., 134 (2012) 101701.

[9] M. M. Salem, M. H. Elhsnawi, S. B. Mohamed, Experimental Investigation of Surface Roughness Effect on Single Phase Fluid Flow and Heat Transfer in Micro-Tube, Int. J. Mech. Mechatron. Eng., 7 (2013) 1821–1825. https://doi.org/10.5281/zenodo.1087810

[10] A. Tamayol, J. Yeom, M. Akbari, M. Bahrami, Low Reynolds number flows across ordered arrays of micro-cylinders embedded in a rectangular micro/minichannel, Int. J. Heat. Mass. Transf., 58 (2013) 420–426. https://doi.org/10.1016/j.ijheatmasstransfer.2012.10.077

[11] Y. Xing, Z. Tao, H. Li, Y. Tian, Experimental investigation of surface roughness effects on flow behavior and heat transfer characteristics for circular microchannels, Chinese. J. Aeronaut., 29 (2016) 1575–1581. https://doi.org/10.1016/j.cja.2016.10.006

[12] B. Markal, O. Aydin, M. Avci, Experimental study of single-phase fluid flow and heat transfer characteristics in rectangular microchannels, Isi Bilim. Ve Tek. Dergisi / J. Therm. Sci. Technol., 38 (2018) 65–72.

[13] R. Kumar, M. Islam, M. M. Hasan, Investigations on Single-Phase Liquid Flow through Semi-Circular Microchannels, Int. J. Appl. Eng. Res., 13 (2018) 6870–6880.

[14] B. Huang, H. Li, S. Xia, T. Xu, Experimental investigation of the flow and heat transfer performance in micro-channel heat exchangers with cavities, Int. J. Heat. Mass. Transf., 159 (2020) 1-10. https://doi.org/10.1016/j.ijheatmasstransfer.2020.120075

[15] S. A. Mohammed E. M. Fayyadh, Effect of artificial cavities on heat transfer and flow characteristics microchannel, IRAQI J. Mech. Mater. Eng., 20 (2020) 180–192. https://doi.org/10.32852/iqjfmme.v20i3.511

[16] M. R. Özdemir, M. M. Mahmoud, T. G. Karayiannis, Flow Boiling of Water in a Rectangular Metallic Microchannel, Heat. Transfer. Eng., 42 (2020) 492-516 . https://doi.org/10.1080/01457632.2019.1707390

[17] S. Kandlikar , S. Garimella , D. Li, S. Colin, M. King , Heat Transfer and Fluid Flow in Minichannels and Microchannels, Editio. Elsevier, 2014.

[18] J.Edward , Jr.Shaughnessy, Introduction to Fluid Mechanics., Oxford universiry press, NY, USA, 2005.

[19] R. K. Shah , A. L .London , Laminar Flow Forced Convection in Ducts. Elsevier,Oxford Acad. Press. Adv. Heat. Transf., (1978). https://doi.org/10.1016/C2013-0-06152-X

[20] A. Koşar, C. J. Kuo, Y. Peles, Boiling heat transfer in rectangular microchannels with reentrant cavities, Int. J. Heat. Mass .Transf., 48 (2005) 4867–4886. https://doi.org/10.1016/j.ijheatmasstransfer.2005.06.003

[21] H. W Coleman , W. G.Steele , Experimentation, Validation, And Uncertainty Analysis For Engineers, Fourth edi. 2018.

[22] R. J. Phillips, Forced-convection, liquid-cooled, microchannel heat sinks, MSc thesis, Massachusetts Institute of Technol. Cambridge, USA, 1987.

[23] M. Mirmanto, Single-phase flow and flow boiling of water in horizontal rectangular microchannels, PhD thesis, Brunel University, London, UK, 2013.

[24] M. R. Özdemir, Single – Phase Flow and Flow Boiling of Water in Rectangular Metallic Microchannels, PhD thesis, Brunel University, London, UK, 2016